Internal calibration of the LUX detector using tritiated methane

D.S. Akerib,[1] H.M. Araújo,[2] X. Bai,[3] A.J. Bailey,[2] J. Balajthy,[4] E. Bernard,[5] A. Bernstein,[6] A. Bradley,[1] D. Byram,[7] S.B. Cahn,[5] M.C. Carmona-Benitez,[8] C. Chan,[9] J.J. Chapman,[9] A.A. Chiller,[7] C. Chiller,[7] T. Coffey,[1] A. Currie,[2] L. de Viveiros,[10] A. Dobi,[4] J. Dobson,[11] E. Druszkiewicz,[12] B. Edwards,[5] C.H. Faham,[13] S. Fiorucci,[9] C. Flores,[14] R.J. Gaitskell,[9] V.M. Gehman,[13] C. Ghag,[15] K.R. Gibson,[1] M.G.D. Gilchriese,[13] C. Hall,[4] S.A. Hertel,[5] M. Horn,[5] D.Q. Huang,[9] M. Ihm,[16] R.G. Jacobsen,[16] K. Kazkaz,[6] R. Knoche,[4] N.A. Larsen,[5] C. Lee,[1] A. Lindote,[10] M.I. Lopes,[10] D.C. Malling,[9] R. Mannino,[17] D.N. McKinsey,[5] D.-M. Mei,[7] J. Mock,[14] M. Moongweluwan,[12] J. Morad,[14] A.St.J. Murphy,[11] C. Nehrkorn,[8] H. Nelson,[8] F. Neves,[10] R.A. Ott,[14] M. Pangilinan,[9] P.D. Parker,[5] E.K. Pease,[5] K. Pech,[1] P. Phelps,[1] L. Reichhart,[15] T. Shutt,[1] C. Silva,[10] V.N. Solovov,[10] P. Sorensen,[6] K. O'Sullivan,[5] T.J. Sumner,[2] M. Szydagis,[14] D. Taylor,[18] B. Tennyson,[5] D.R. Tiedt,[3] M. Tripathi,[14] S. Uvarov,[14] J.R. Verbus,[9] N. Walsh,[14] R. Webb,[17] J.T. White,[17] M.S. Witherell,[8] F.L.H. Wolfs,[12] M. Woods,[14] and C. Zhang[7]

[1] *Case Western Reserve University, Dept. of Physics, 10900 Euclid Ave, Cleveland OH 44106, USA*
[2] *Imperial College London, High Energy Physics, Blackett Laboratory, London SW7 2BZ, UK*
[3] *South Dakota School of Mines and Technology, 501 East St Joseph St., Rapid City SD 57701, USA*
[4] *University of Maryland, Dept. of Physics, College Park MD 20742, USA*
[5] *Yale University, Dept. of Physics, 217 Prospect St., New Haven CT 06511, USA*
[6] *Lawrence Livermore National Laboratory, 7000 East Ave., Livermore CA 94551, USA*
[7] *University of South Dakota, Dept. of Physics, 414E Clark St., Vermillion SD 57069, USA*
[8] *University of California Santa Barbara, Dept. of Physics, Santa Barbara, CA, USA*
[9] *Brown University, Dept. of Physics, 182 Hope St., Providence RI 02912, USA*
[10] *LIP-Coimbra, Department of Physics, University of Coimbra, Rua Larga, 3004-516 Coimbra, Portugal*
[11] *SUPA, School of Physics and Astronomy, University of Edinburgh, Edinburgh, EH9 3JZ, UK*
[12] *University of Rochester, Dept. of Physics and Astronomy, Rochester NY 14627, USA*
[13] *Lawrence Berkeley National Laboratory, 1 Cyclotron Rd., Berkeley, CA 94720, USA*
[14] *University of California Davis, Dept. of Physics, One Shields Ave., Davis CA 95616, USA*
[15] *Department of Physics and Astronomy, University College London, Gower Street, London WC1E 6BT, UK*
[16] *University of California Berkeley, Department of Physics, Berkeley, CA 94720, USA*
[17] *Texas A & M University, Dept. of Physics, College Station TX 77843, USA*
[18] *South Dakota Science and Technology Authority, Sanford Underground Research Facility, Lead, SD 57754, USA*

We describe the development, deployment, and exploitation of a tritium calibration source for the LUX dark matter experiment. The source is useful for calibrating the electron recoil backgrounds over the full volume of the detector, and for characterizing the behavior of the LUX TPC. We report on the LUX electron recoil discrimination factor, the detector threshold, and on the detector physics of liquid xenon at the LUX electric field value of 181 V/cm.

I. Introduction

The LUX collaboration recently reported results from its first underground science run, placing new constraints on WIMP dark matter with masses between 6 GeV and 1 TeV[1]. LUX is a large dual-phase liquid xenon (LXe) time projection chamber (TPC) with an active mass of 270 kg. The primary scintillation light from particle interactions (S1) is collected by two arrays of photomultiplier tubes (PMTs) at the top and bottom of the detector, and the charge signal is converted to light via secondary scintillation at the anode (S2). Measurement of both S1 and S2 allows the event to be located in all three dimensions, and allows discrimination between nuclear recoil (NR) events and electron recoil (ER) events via the ratio (S2/S1).

One of the primary advantages of the liquid TPC technology is its high efficiency for the rejection of external gamma backgrounds via self-shielding. On the other hand, self-shielding also reduces the effectiveness of external gamma calibration sources such as ^{137}Cs or ^{228}Th , particularly in the center of the detector and at the low energies relevant for dark matter searches. In the case of LUX, external gamma sources are unable to produce a useful rate of ER calibration events in the

fiducial region.

To address this issue, internal calibration sources can be dissolved into the liquid xenon and thereby defeat its self-shielding have been developed [2]. LUX has deployed two such internal calibration sources; the first based upon ^{83m}Kr , and the second based upon tritium (^{3}H). ^{83m}Kr is a source of two internal conversion electrons at energies of 9.4 keVee and 32.1 keVee separated in time by an intermediate state with a half life of 154 ns[3][4]. Because it produces two lines in the energy spectrum, ^{83m}Kr is suitable for tracking the spatial and time dependence of the S1 and S2 signals. However, because both ^{83m}Kr electrons are above the energy range of interest for dark matter (0.9 - 8 keVee), and because the S2 signals from the two electrons generally overlap with each other in the detector, ^{83m}Kr is less useful for constraining the electron recoil (ER) band of the S2/S1 discriminant.

In this article we describe the development and use of the LUX tritium source, which plays a complementary role to the ^{83m}Kr source. Unlike ^{83m}Kr , tritium is a single-beta emitter, with a Q value of 18.6 keVee [5]. Its spectral mean beta energy is 5.6 keV [6] peaking at 3.0 keVee, and 75% of its beta decays are below 8 keVee [7]. This allows the detector's ER band to be precisely characterized throughout the full volume of the detector and allows the threshold response of the detector to be studied.

Unlike ^{83m}Kr , however, tritium is long-lived, with a half-life of 12.3 years[8] (compared to 1.8 hours for ^{83m}Kr), so the tritium must be removed from the liquid xenon by purification. Secondly, tritium must be introduced into the detector in a manner which will not impair the charge or light collection properties of the detector. This is less of a concern with ^{83m}Kr , both because krypton is a noble element, and because spectator electronegative impurities intrinsic to the source may be removed by passing the krypton through the LUX getter prior to entering the detector. Tritium, on the other hand, is removed by the getter, and must therefore be introduced downstream.

Tritiated methane (CH_3T) was chosen as the appropriate host molecule to deliver the activity into LUX. Methane has several desirable chemical and physical properties compared to T_2: first, its diffusion constant (D) times solubility (K) at room temperature is ten times smaller in common LUX materials such as teflon (PTFE) and polyethylene (PE)[9], mitigating the problem of back-diffusion of activity into the liquid xenon after purification; it is chemically inert, so it is not expected to adhere to surfaces (as the T_2 molecule is known to do), and it is consistent with maintaining good charge transport in liquid xenon.

In developing and deploying the source, our purification goal was that any residual activity that remained due to back-diffusion from plastics or from inefficient purification should be no more than 0.33 μBq, which is 5% of the LUX ER background rate design goal for a 30,000 kg·days exposure. We desired to collect a LUX calibration dataset of ∼15,000 tritium events, roughly a factor of 100 larger than the number of expected ER background events in LUX [10] .

This article is organized as follows. In Section **??**, we describe the bench-top purification tests and calculations that we employed to verify the suitability of the tritiated methane source for injection and removal from LUX. In Section **??** we describe the analysis of the tritium decay data collected by LUX and its implications for our WIMP dark matter search.

II. Development of the Calibration Source

1. Tritiated Methane Removal

The removal efficiency of zirconium getters for methane in xenon had previously been studied at the University of Maryland. It was found that greater than 99.99% of natural methane can be removed in a single pass through a zirconium getter. [11] Tritiated methane is chemically identical to natural methane, so it follows that similar removal efficiencies should be expected for CH_3T. To verify this a small scale tritiated methane injection system was integrated into a liquid xenon system at the University of Maryland. This system used a SAES MC1-905F methane purifier placed in series immediately after the CH_3T source bottle to prevent non-methane species of tritium from entering the plumbing. Over 68,000 Bq of observed CH_3T activity was injected into this small scale system and a removal efficiency of over 99.99% for tritiated methane in xenon was confirmed.

2. Out Gassing of Tritiated Methane from Plastics

An accurate model of a tritiated methane injection into LUX must account for out gassing of CH_3T from plastics such as polyethylene and teflon. Using data from the liquid xenon experiments at the University of Maryland we numerically modeled the purification and residual diffusion of CH_3T in the detector. Using Duhamel's priciple, an integral solution to Fick's

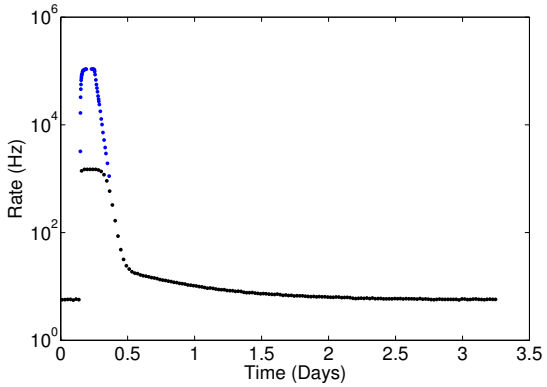

FIG. 1: A time histogram of the event rate during a tritium injection into our small scale detector. The event rate greatly exceeded the limits of our ADC (black data points), so a analog scalar was used to count the true event rate (blue data points).

second law on a half-infinite line can be found to be

$$\phi(x,t) = KC_{out} - \int_0^t erf(\tfrac{x}{\sqrt{4D(t-\tau)}})KC\dot{}_{out}(\tau)d\tau - KC_{out}(0)erf(\tfrac{x}{\sqrt{4Dt}}),$$

where K is the solubility of the material, D is the diffusion constant, and C_{out} is the concentration at the surface of the material. For the out gassing process we are only able to detect the flux of material out of the plastic. This is given by Fick's first law evaluated at $x = 0$,

$$J_{out}(t) = -K\sqrt{\frac{D}{\pi}}\left(\int_0^t \frac{C\dot{}_{out}(\tau)}{\sqrt{t-\tau}}d\tau + \frac{C_{out}(t)}{\sqrt{t}}\right),$$

where the sign has been flipped since the flux of material is outward. We see that it is no longer possible to evaluate K and D separately, since the diffusion in and out of the plastic is completely determined by the time-dependent concentration outside of the plastic. To simplify our model, we define a new constant

$$G = K\sqrt{\frac{D}{\pi}}.$$

By fitting the integral of the flux out of the plastic over time to out gassing data collected in Maryland's liquid xenon system we constrain $G \leq 0.0075\ \frac{cm}{\sqrt{day}}$.

With a constraint on G taken from the analytic solution to Fick's second law, we turn to numerical simulation to answer the question of how much initial CH_3T activity to inject into LUX to meet our calibration conditions. Several assumptions are made to simplify the numerical model. First, we approximate the diffusion into plastic as being a one dimensional process. Since the plastic in our detector at Maryland and in LUX can be approximated by a cylindrical shell, there is no dependence on the azimuthal or z coordinates. Since r is large compared to the thickness of the plastic shell, $\frac{\delta^2\phi}{\delta r^2} \gg \frac{1}{r}\frac{\delta\phi}{\delta r}$, so Fick's laws in a one dimensional approximation become

$$J = -D\frac{\delta\phi}{\delta r}\vec{r}$$

$$\frac{\delta\phi}{\delta t} = D\frac{\delta^2\phi}{\delta r^2}.$$

We assume the concentration of CH_3T in LUX is uniform throughout its volume, since the design of LUX creates currents which stir the liquid xenon. With perfect mixing the effect of the purifier can be modeled by adding an exponential time dependence to the outer volume. The time constant of this decay has an upper limit equal to the time it takes xenon to recirculate through the LUX detector, although in reality the mass transport from diffusion in the liquid and gaseous xenon decreases this time constant.

We use a simple implementation of the first order Euler method for our numerical simulations. The diffusion is simulated by setting the concentration at the boundary of the piece equal to KC_{out}, where C_{out} is the concentration of CH_3T in the xenon. This concentration is dependent on time according to

$$\frac{\delta C_{out}}{\delta t} = J_{out}\frac{A_{plastic}}{V_{xenon}} - \frac{C_{out}}{\tau},$$

where $A_{plastic}$ is the surface area of the plastic cylinder, V_{xenon} is the total volume of xenon in the fiducial region, and τ is the characteristic removal time of methane from LUX (with perfect mixing and purification efficiency, this will be identical to the turnover time of xenon in LUX, but purifier inefficiencies and Henry's Law solubilities can have a significant effect on this value). The first term on the right of this equation models out gassing of CH_3T from the plastic cylinder, while the second term models removal of CH_3T through purification. Using the first order Euler method, we arrive at an expression for C_{out} given by

$$C_{j+1} = C_j + \Delta t\left[(J_{1,j} - J_{N_x,j})\frac{A_{plastic}}{V_{xenon}} - \frac{C_j}{\tau}\right].$$

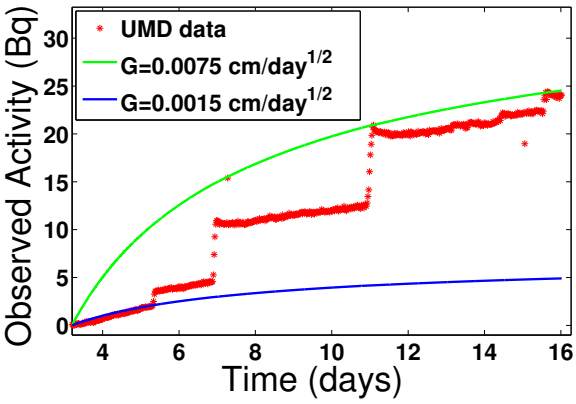

FIG. 2: This plot shows the tritium activity observed after an injection into the small scale detector at Maryland. There were several polyethylene panels placed in the liquid xenon during this injection, and after about 3.5 days, the getter was put into bypass mode and the activity began to rise. The blue curve shows the upper limit of G which accounts for the steps seen in the data (the red points). The green curve, which shows the lower limit, assumes that these steps are not due to the outgassing from the PE panels and only fits to data before the first jump.

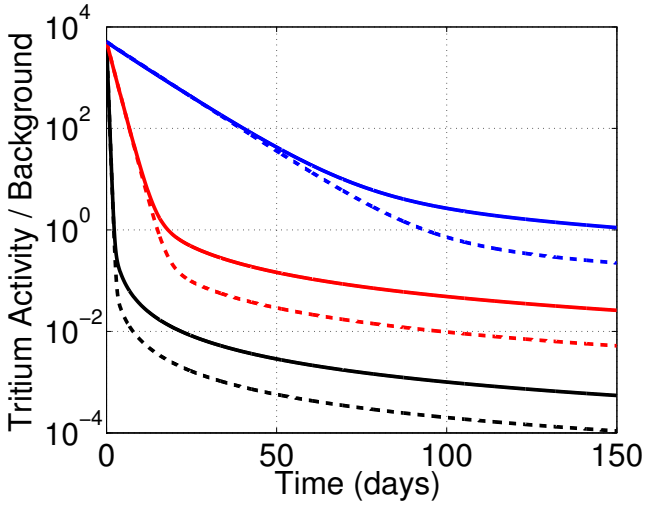

FIG. 3: Displayed are the results of simulated 0.1 Bq injections of tritiated methane into LUX. The dashed curves assume the lower limit of G (0.0015 cm/day$^{1/2}$, while the solid curves assume the upper limit of G (0.0075 cm/day$^{1/2}$). The black curves assume a characteristic removal time of 0.25 days, the black curves assume 1.7 days, and the blue curves assume 10 days.

The initial concentration is defined by dividing the desired injection activity by the volume of the fiducial region. We choose $D = 2.3 \times 10^{-9} \frac{cm^2}{sec}$ so that the half-infinite boundary conditions in our diffusion model is valid, and combine this with our allowed range of values for G to extract a value for K. We use this model to predict the total number of calibration events as well as the time required to return to <5% of the nominal background rate for any CH_3T injection into LUX.

III. Implementation of the Calibration Source

1. Injection System Hardware

The setup of our triated methane calibration technique can be separated into three parts: the tritiated methane source bottle, the injection system, and the zirconium getter.

The tritiated methane source bottle for our calibration technique consists of a 2250 cc stainless steel bottle which is filled with a mixture of tritiated methane and purified xenon. The purpose of this xenon is to serve as a carrier gas for the tritiated methane. The total activity in the source bottle is set by mixing tritiated methane from a reservoir into the source bottle via volume sharing.

The injection system for our tritiated methane calibration technique consists of a series of expansion volumes which are used to fine tune the amount of CH_3T that is injected. Once the CH_3T source bottle is opened it flows through a methane gas purifier (SAES MC1-905F) to remove any non-methane species of tritium, such as bare tritium. The expansion volumes are then filled with tritiated methane from the source bottle, and the flow of xenon in the gas system is diverted through the expansion volumes to sweep the CH_3T into the detector downstream of the LUX xenon purifier. A pump out port allows the expansion volumes to be evacuated in preparation for each use of the injection system.

The LUX gas system uses a hot zirconium getter (SAES-PS4MT15R1) located upstream of the CH_3T injection system to remove CH_3T from the xenon after passing through the detector.

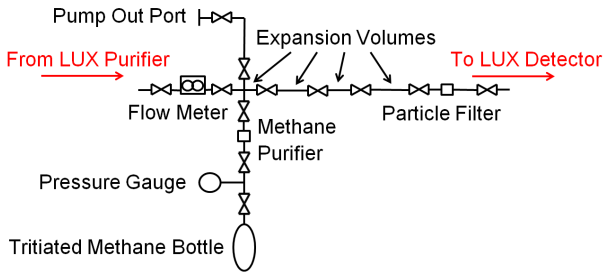

FIG. 4: Plumbing diagram of the tritium injection system for LUX. Tritium is injected downstream of the LUX xenon purifier so that it passes through the detector once prior to being removed. Red arrows indicate the direction of flow.

IV. Results from the Tritiated Methane Calibration

1. Tritiated Methane injection into the LUX detector

In the experimental setup at UMD it was demonstrated that tritiated methane could be injected directly into a liquid xenon vessel containing plastics and removed. However, even with conservative estimates of diffusion rates into mock plastic components we could not be certain about the diffusion of methane in the much larger LUX detector. Having an integrated xenon gas sampling system, developed for LUX to monitor krypton daily [12] [13], allowed us to conduct situ methane measurements providing a diagnostic of the natural methane diffusion without the risk of permanent tritium contamination. Before injecting tritiated methane into the detector we first injected $1/10^6$ (g/g) of natural methane and demonstrated its removal from the LUX xenon to five orders of magnitude, this allowed us to proceed with confidence knowing that the goal of reducing the tritium rate to less than 5% of background could be met. Methane is chemically identical to tritiated methane and having the ability to sample the gas proved useful for the tritium campaign, the purification time constant for natural methane removal was measured to be 5.9 ± 0.07 hours with the xenon gas sampling system 5. The removal time constant was 1/5 of that expected based on xenon circulation rates alone, potentially enhanced by the solubility of methane between the liquid and gaseous xenon. The enhanced purification time constant allowed for larger injections of tritiated methane into the detector.

Following the natural methane test the tritiated methane injection was conducted. An absolute activity of 20 mBq of tritiated methane was injected at the purifier's outlet while circulating. A removal time constant of 6.0 ± 0.5 hours was measured in the liquid volume, consistent with the natural methane removal measured in the gas by the sampling system 7. After a day of circulating through the getter the tritium rate had fallen below detectable levels confirming the effective removal of the tritiated methane with the getter. A second, larger injection of 800 mBq was performed a week later yielding a similar removal time constant of 6.4 ± 0.1. The second injection produced 20,000 beta decays in the LUX detector before being completely removed, 7000 of which were in the fiducial volume and could used to calibrate the ER band in the WIMP search region of 1-50 Phe (about 1-8 keVee). The new tritium calibration source provided an unprecedented low energy electronic recoil calibration for the LUX dark matter search [1]. The injections were performed while circulating and with the getter actively purifying in order maintain detector purity and stability. Prior to LUX detector upgrades in December of 2013 a total of 10 Bq of tritiated methane was injected into the LUX detector and successfully removed providing over 150,000 beta decays within the fiducial volume.

In addition to providing a direct measure of the removal rate of methane from LUX, the natural methane injection allowed a stronger and more direct limit to be placed on the outgassing from the plastics. As seen in figure **??**, the highest value allowed for the outgassing constant is 0.0016 cm/day$^{1/2}$, which is in agreement with the lower limit discussed in section 2. We call this an upper limit because the apparent elbow observed in the data occurs at the sensitivity limit of the sampling system. With the measurement of both the outgassing constant, and the removal rate of methane, it is now possible to place strong limits on the time cost of performing a tritiated methane calibration, as shown in figure 6.

2. Mixing of Tritiated Methane in Liquid Xenon

Tritium events appear uniformly distributed in the liquid volume several minutes after injecting the tritiated methane inline with the xenon gas circulation path. Figure 8 shows the R^2 vs. Z distribution of tritium events thirty minutes after an injection. The events shown cover the region from the gate to the cathode and radially outward to the edge of the detector. An additional cut requiring that the event be between $\pm 3\sigma$ of the ER mean was made to disregard residual alpha events from the walls and cathode, the event rate consisted overwhelmingly of tritium events. The tritiated methane dispersed uniformly

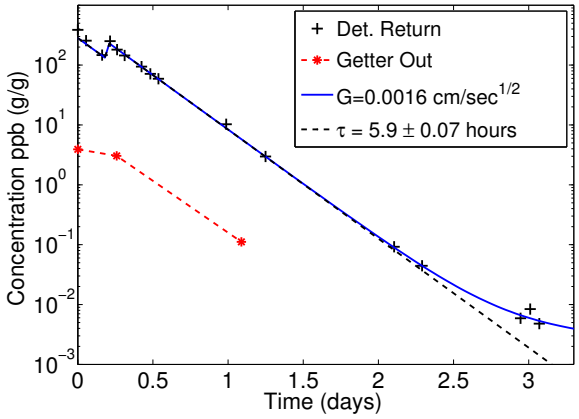

FIG. 5: Removal of natural methane observed by the integrated xenon sampling system prior to the tritiated methane injections. The red points indicate measurements at the getter outlet, we find a 97% one pass removal efficiency at a flow rate of 25 SLPM. The blue curve shows the improved upper limit on the effect of outgassing from the plastics. The black dashed lines shows the exponential fit to the natural methane removal from the xenon with a time constant of 5.9 ±0.07 hours. 5×10^{-3} ppb (g/g) is the limit of detection for methane.

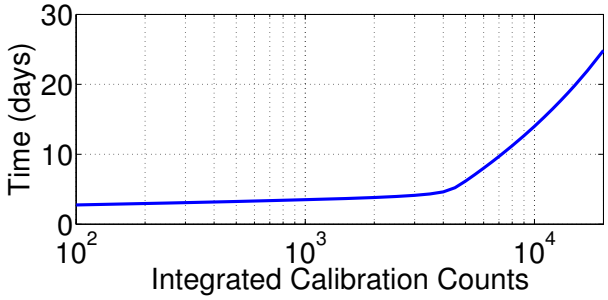

FIG. 6: Shown above is the time required to allow the tritium activity to fall to $< 5\%$ of the nominal LUX background, calculated using the purification rate and outgassing constant measured during the natural methane injection.

throughout the liquid xenon illuminating all regions on the detector.

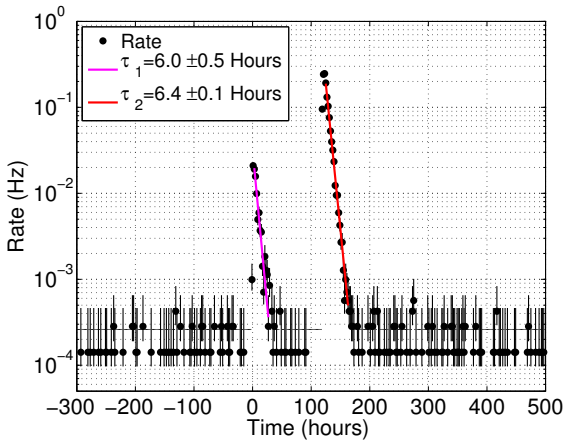

FIG. 7: Left: Rate of single scatter events with S1 below 150 Phe in the fiducial volume. 150 Phe in S1 is about 18.6 keVee, the endpoint to the tritium beta spectrum. The magenta and red curves are fits to the first and second tritium injection's removal rate. Right: The rate of single scatter events with S1 below 150 for the whole detector volume. Note the removal of tritiated methane is consistent with the natural methane removal rate measured independently.

3. Definition of Electronic Recoil Band and Comparison with NEST Model

The electronic recoil band in the fiducial volume of the LUX detector was calibrated to unprecedented accuracy using the tritium source. Figure 9 shows the tritium calibration data with fits to the mean of the ER band along with the 10-90% confidence bounds ($\pm 1.28\sigma$), at a drift field of 180 V/cm. The values of the leakage fraction at 50% NR acceptance per each 1 Phe bin in S1 are shown in 10. The nuclear recoil band, in red, is defined by the NEST model along with AmBe and ^{252}Cf calibrations. The amount of methane injected to perform the calibration was less than 1 part-per-trillion ($< 10^{-12}$) far to small to cause degradation in electron lifetime or quench xenon scintillation [14]. We have also independently verified the null impact on electron lifetime and light yield by performing a tritiated methane while taking ^{83m}Kr calibration data [cite, thesis].

WIMPs primarily interact with the atomic nuclei of xenon atoms in LUX resulting in nuclear recoils whereas the vast majority of residual radioactivity within the detector are gammas

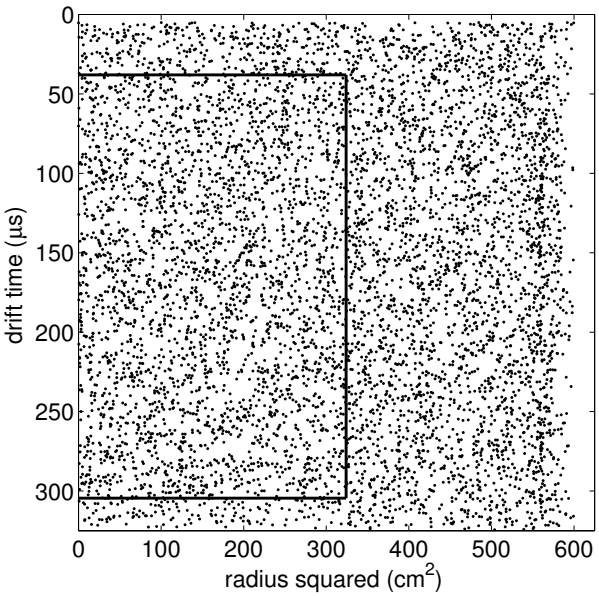

FIG. 8: The distribution of tritium events vs. detector radius squared. The solid black line represents the fiducial volume.

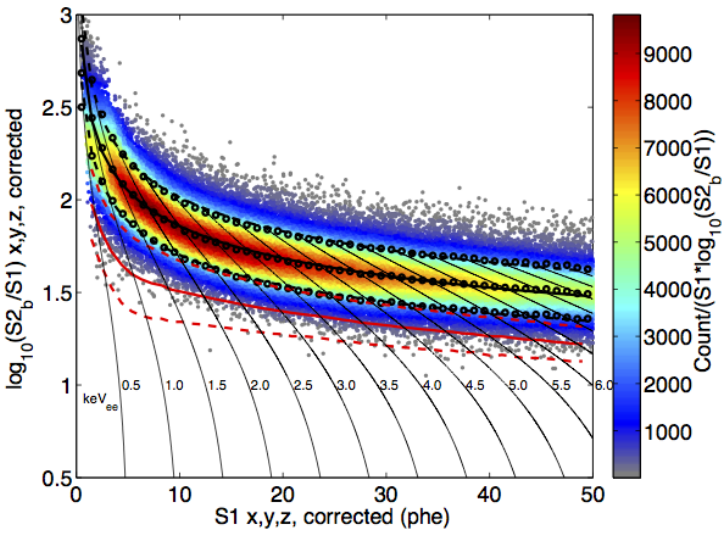

FIG. 9: Discrimination vs. S1 using over 115,000 tritium beta decays between 1 and 50 Phe in S1 (about $1 - 8\text{keV}_{ee}$). On average from 1 to 30 Phe the discrimination is 99.58%, defined by the fraction of events of events below the mean of the nuclear recoil band. The red band represents the NEST nuclear recoil band (version 0.98) vetted with an AmBe, ^{252}Cf and DD neutron generator calibration.

which result in electronic recoils. Thus, knowing the separation of the ER from the NR band allows for a measure of the background rejection figure of merit for a liquid xenon experiment. We define the background rejection figure of merit as leakage fraction, reported here as the fraction of ER events that leak into the lower half of the NR band. Over 115,000 tritium decays were used for the ER band calibration, between 1-50 Phe in S1 (1-8 keV$_{ee}$), and were found using standard WIMP search cuts within the fiducial volume. Figure 10 shows the leakage fraction per 1 Phe bins of S1. The mean leakage fraction in the region used for the LUX 2013 PRL results, between 1-30 Phe (1-5 keV$_{ee}$) in the fiducial, was found to be 0.42% $\pm$ 0.02%, see Figure 10. Figure 11 shows the reconstructed energy spectrum for those tritium events in the fiducial volume of the detector (black) along with the tritium spectrum from NEST modeling (blue) and an ideal tritium spectrum (magenta). The reconstructed energy matches the tritium beta spectrum well from 1 to 18 keV$_{ee}$. The calibration data was acquired in a 40 hour time window in which less than three out of 115,000 events are expected to be non tritium [10], this implies a near perfect data purity for the calibration. Nearly every point (99.997%) show in figure 9 and the histogram of 11 is the result of a tritium beta decay in the fiducial volume of the LUX detector.

4. Threshold Determination

The tritiated methane calibration source provides beta decays with energies down to 0.1 keV$_{ee}$ allowing for an independent measure the LUX detector's threshold. The limitation for detecting a single scatter WIMP like event event with PMTs is the S1 (primary scintillation) signal, being more than an order of magnitude less than the S2 signal. The S1 threshold could be measured by comparing the NEST model, assuming perfect detector resolution, to the observed tritium beta spectrum from 0.1-10 keV$_{ee}$. The threshold determined by comparing the tritium data to NEST is in good agreement with all other methods used for determining the threshold in the LUX detector, figure 12.

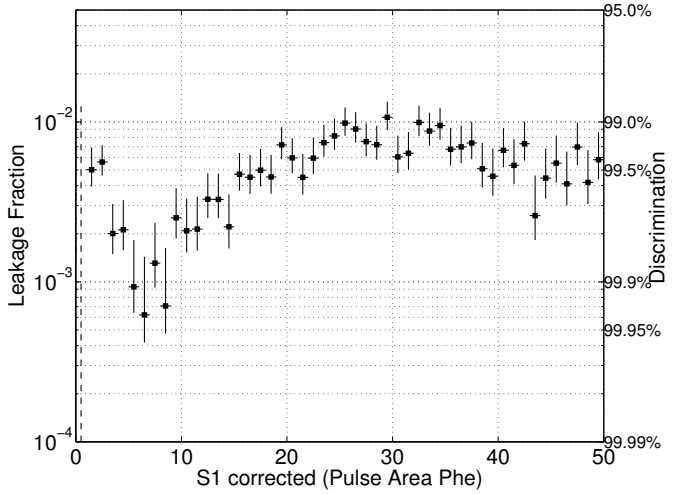

FIG. 10: Discrimination vs. S1 using over 115,000 tritium beta decays between 1 and 50 Phe in S1 (about $1-8\text{keV}_{\text{ee}}$). On average from 1 to 30 Phe the discrimination is 99.58%, defined by the fraction of events of events below the mean of the nuclear recoil band. The red band represents the NEST nuclear recoil band (version 4c) vetted with an AmBe, ^{252}Cf and DD neutron generator calibration.

V. Additional Calibrations with Tritium

In this paper we have described the development and use of a tritiated methane calibration source for large scale xenon detectors. The primary application of the tritiated methane calibration source is to characterize the ER band and measure discrimination from electronic and nuclear recoils. However, much more fundamental xenon physics can be probed with the tritium calibration source. With higher statistics the discrimination can be measured in finer bins of energy or S1 Phe (figure 10) along with the Gaussianity of the ER band. The log(S2/S1) has been assumed to have Gaussian behavior in past experiments, never before has there been an ER calibration with such high data purity in the WIMP search region to observe potential non-Gaussian behavior. The largest tritium calibration in LUX detector's fiducial region produced 115,000 tritium beta decays with only three being non tritium events. The tritium calibration can also used to calculate the light yield, charge yield and recombination fluctuation over the range from 1 to 18 KeV_{ee}. The current data taken with the LUX detector has allowed for the vetting of the NEST model

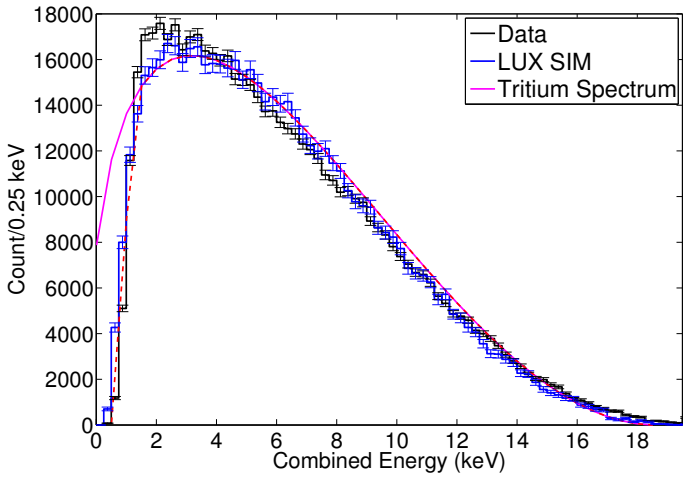

FIG. 11: Energy histogram of tritium events. The black histogram represents the data, in blue is the tritium spectrum produced with LUX SIM based on NEST. The magenta curve shows the true tritium beta spectrum without smearing due to finite detector resolution, the dashed line indicates the true tritium spectrum convolved with the threshold

down to 1 keV_{ee} for the first time. Finally, tritium provides a low energy uniformly distributed source making it ideal for determining the fiducial volume of a detector and calibrating position reconstruction algorithms for low energy events.

VI. Summary

We have presented our new technique for injecting and removing CH_3T as an internal calibration source in detectors which utilize liquid and gas phase noble gases. We discussed the assembly of our CH_3T calibration system, motivated by gas and liquid phase R&D experiments at the University of Maryland. We have used data from the LUX detector to show that our system can safely inject CH_3T for the purpose of internal calibration.

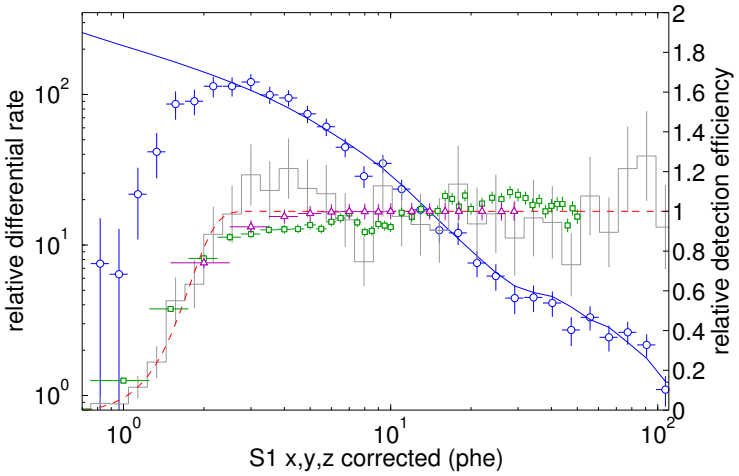

FIG. 12: Comparison of AmBe data (blue circles) with NEST simulations (blue line), showing excellent agreement above the 2 phe threshold (left axis). The gray histogram and fitted dashed red line show the relative efficiency for detection of nuclear recoils from AmBe data (right axis). Overlaid are the ER detection efficiency from tritium data (green squares), applied to the ER background model in the profile likelihood analysis, and the efficiency from full detector NR simulations treated as real data in terms of the digitized MC-truth S1 phe (purple triangles), applied to the WIMP signal model. The efficiency calculation here does not include S1 or S2 area thresholds.

[1] S. Akerib, D. et al. First results from the lux dark matter experiment at the sanford underground research facility. *Phys. Rev. Lett.*, 112:091303, Mar 2014. doi: 10.1103/PhysRevLett.112.091303.

[2] L.W. Kastens, S. Bedikian, S.B. Cahn, A. Manzur, and D.N. McKinsey. A 83Krm Source for Use in Low-background Liquid Xenon Time Projection Chambers. *JINST*, 5:P05006, 2010. doi:10.1088/1748-0221/5/05/P05006.

[3] I. Ahmad, et al. Half-lives of isomeric states in fe57 and kr83. *Phys. Rev. C*, 52:2240–2241, Oct 1995. doi: 10.1103/PhysRevC.52.2240.

[4] S. L. Ruby, Y. Hazoni, and M. Pasternak. Lifetimes of the low-energy m1 transitions in la137 and kr83. *Phys. Rev.*, 129:826–828, Jan 1963. doi:10.1103/PhysRev.129.826.

[5] Sz. Nagy, T. Fritioff, M. Bjrkhage, I. Bergstrm, and R. Schuch. On the q -value of the tritium ?-decay. *EPL (Europhysics Letters)*, 74(3):404, 2006.

[6] D. P. Gregory and D. A. Landsman. Average decay energy of tritium. *Phys. Rev.*, 109:2091–2091, Mar 1958. doi: 10.1103/PhysRev.109.2091.

[7] P Venkataramaiah, K Gopala, A Basavaraju, S S Suryanarayana, and H Sanjeeviah. A simple relation for the fermi function. *Journal of Physics G: Nuclear Physics*, 11(3):359, 1985.

[8] L. L. Lucas and M. P. Unterweger. Comprehensive review and critical evaluation of the half-life of tritium. *Journal of Research of NIST*, 105(4):541 – 551, 2000. ISSN 0883-2889. doi:http://dx.doi.org/10.6028/jres.105.043.

[9] Hitoshi Miyake, Masao Matsuyama, Kan Ashida, and Kuniaki Watanabe. Permeation, diffusion, and solution of hydrogen isotopes, methane, and inert gases in/through tetrafluoroethylene and polyethylene. *Journal of Vacuum Science Technology A:*

Vacuum, Surfaces, and Films, 1(3):1447–1451, Jul 1983. ISSN 0734-2101. doi:10.1116/1.572038.

[10] D. S. Akerib, et al. Radiogenic and Muon-Induced Backgrounds in the LUX Dark Matter Detector. *ArXiv e-prints*, March 2014.

[11] A. Dobi, et al. Study of a zirconium getter for purification of xenon gas. *Nuclear Instruments and Methods in Physics Research Section A: Accelerators, Spectrometers, Detectors and Associated Equipment*, 620(23):594 – 598, 2010. ISSN 0168-9002. doi:http://dx.doi.org/10.1016/j.nima.2010.03.151.

[12] Attila Dobi, et al. Detection of krypton in xenon for dark matter applications. *Nucl.Instrum.Meth.*, A665:1–6, 2011. doi: 10.1016/j.nima.2011.11.043.

[13] A. Dobi, et al. Xenon purity analysis for EXO-200 via mass spectrometry. *Nucl.Instrum.Meth.*, A675:40–46, 2012. doi: 10.1016/j.nima.2012.01.066.

[14] K. N. Pushkin, et al. Scintillation light, ionization yield and scintillation decay times in high pressure xenon and xenon methane. *Nuclear Science, IEEE Transactions on*, 54(3):744–750, June 2007. ISSN 0018-9499. doi: 10.1109/TNS.2007.894815.